Volume 16
Number 3
9 February 2026
Pages 669–1060

Catalysis Science & Technology

rsc.li/catalysis

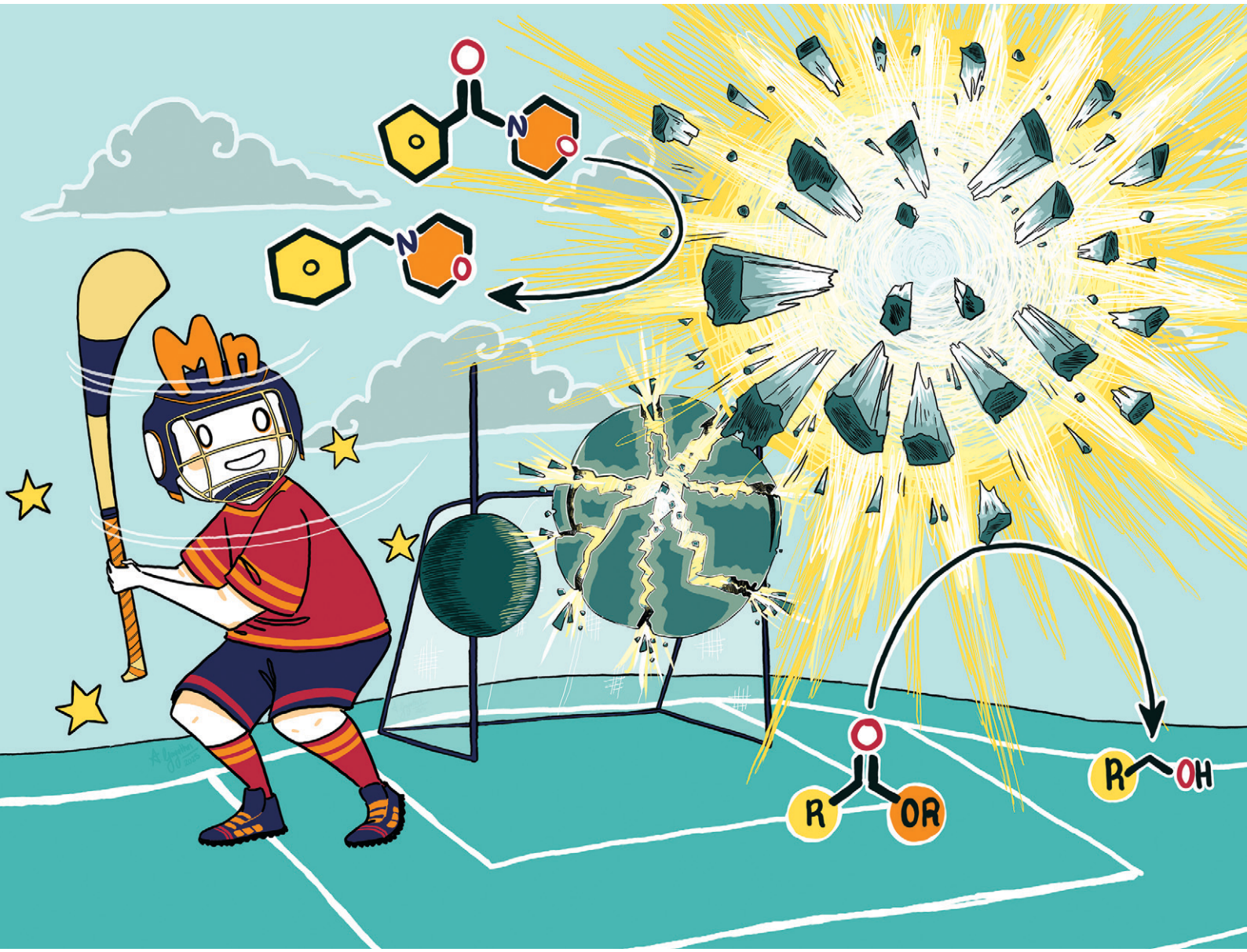

ISSN 2044-4761

ROYAL SOCIETY OF CHEMISTRY

PAPER

Ian J. S. Fairlamb, Jason M. Lynam, Gerard P. McGlacken *et al.*
Polymer-supported manganese-catalysed transformation of esters and aldehydes to alcohols

Catalysis Science & Technology

ROYAL SOCIETY OF CHEMISTRY

PAPER

View Article Online
View Journal | View Issue

Cite this: *Catal. Sci. Technol.*, 2026, **16**, 821

Polymer-supported manganese-catalysed transformation of esters and aldehydes to alcohols

V. Kishore Kumar Pampana, [a] Si Lok Ko,[a] Eimear Courtney,[a] Benjamin R. O'Donoghue, [a] David J. Jones, [a] Simon K. Beaumont, [b] Davinder Singh,[c] Charlotte Willans, [d] Ian J. S. Fairlamb, *[d] Jason M. Lynam *[d] and Gerard P. McGlacken *[a]

Received 1st October 2025,
Accepted 12th November 2025

DOI: 10.1039/d5cy01174d

rsc.li/catalysis

Compared to precious metals, manganese has emerged as a more earth-abundant and potentially safer metal to catalyse important chemical transformations. In contrast to homogeneous Mn catalysts, the use of heterogeneous Mn catalysts, is rare. Herein we describe the preparation of a Mn catalyst supported on a simple phosphine-containing polymer, that efficiently provides alcohols from esters and aldehydes, and facilitates the reduction of amides. Surprisingly, the catalyst gave improved yields upon recycling, which prompted a short study into the structural and oxidative changes of the catalyst using SEM-EDX and XAFS. Breakage of the microspheres and increased Mn oxidation states were observed upon recycling. Ultimately a priming procedure was developed that enabled direct procurement of an active and viable catalyst system.

Introduction

In recent decades, the field of catalysis has been largely dominated by complexes of late transition metals, including palladium (Pd), ruthenium (Ru), iridium (Ir), and platinum (Pt).[1] However, non-precious metals offer greater natural abundance, often lower toxicity and the potential for new and exciting catalytic behaviour and reaction outcomes. Manganese-based catalysts have garnered significant attention in catalysis due to the earth-abundance of Mn (12th most abundant in the earth's crust) and the cost-effectiveness of the raw material.[2] Additionally, Mn is usually considered less toxic compared to many other transition metals.[3] Indeed Mn is essential for numerous biochemical processes in the human body[4] and is potentially a more sustainable and environmentally friendly choice for catalytic applications.[5] Mn has emerged as a versatile and well-studied metal in homogeneous catalysis, with numerous reports highlighting its application across a wide variety of reactions.[6–10]

The reduction of organic molecules is crucial in synthesis, and manganese has served as an efficient but rather underutilised catalyst, for these transformations.[11] There has been a notable rise in manganese-mediated reduction reactions using silanes as a substitute for hydrogen, highlighting a shift towards safer approaches in catalytic processes.[12–17]

Heterogeneous catalysis plays a prominent role in modern organic synthesis and many other areas of the chemical industry.[18] Its widespread application derives from overall efficiency and recyclability, making it a key approach for sustainable chemical transformations.[19–23] There have been a few reports on the use of polymer-supported, earth-abundant metals, as catalysts.[24] For example, Vimal *et al.* reported a novel polystyrene divinylbenzene-supported Fe(III) catalyst for hydrogenation.[25] Yamada developed a poly(4-vinylpyridine)-supported Co(II) catalyst for regioselective [2 + 2 + 2] cyclotrimerization of terminal aryl alkynes.[26] In 2025, Lin *et al.* reported a unique porous organic polymer-supported chiral Co catalyst for asymmetric C–H functionalization,[27] and the Ding group developed a phosphine oxide containing porous organic polymer-supported Co catalyst for 2-octene hydroformylation.[28] Polymer supported manganese catalysts have also displayed some success,[29–32] but overall, the area of polymer supported earth-abundant metals in catalysis is in its infancy.

[a] *School of Chemistry, Analytical and Biological Chemistry Research Facility (ABCRF), University College Cork, T12 YN60, Ireland. E-mail: g.mcglacken@ucc.ie*
[b] *Department of Chemistry, Durham University, South Road, Durham, DH1 3LE, UK*
[c] *Tyndall National Institute, Cork T12 R5CP, Ireland*
[d] *Department of Chemistry, University of York, Heslington, York, YO10 5DD, UK. E-mail: ian.fairlamb@york.ac.uk, jason.lynam@york.ac.uk*

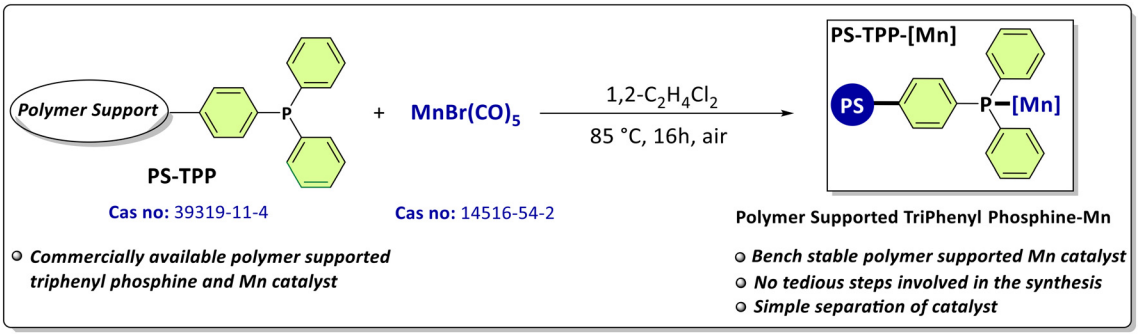

Scheme 1 Synthesis of heterogeneous Mn catalyst.

Results and discussion

We aimed to develop a manganese-based heterogeneous catalyst that is easy to synthesize using readily available materials. By analogy with Angelici and Basolo's work on the synthesis of homogeneous Mn catalysts,[33] we mixed a commercially available polymer-supported triarylphosphine ligand with $MnBr(CO)_5$ in 1,2-dichloroethane (DCE) at 85 °C for 16 hours under air (Scheme 1), to generate a novel heterogeneous Mn catalyst (PS-TPP-**[Mn]**). The Mn content determined by ICP-OES for this fresh catalyst (for more details, see the SI) implies a Mn loading of 7 wt%, which pleasingly corresponds to binding of 80% of the polymer-bound triarlyphosphines. This catalyst stands out from the few existing heterogeneous Mn catalysts[29–32] as it can be synthesized in a single step using readily available reagents, involves very simple separation and isolation, and appears bench stable.

Fourier transform infrared spectroscopic analysis (FTIR) enabled preliminary confirmation of the structure of the synthesized heterogeneous Mn catalyst (Fig. 1). The FTIR analysis of the commercially available $MnBr(CO)_5$ complex (Fig. 1 top) shows the expected carbonyl peaks (2137 cm^{-1}, 2081 cm^{-1}, 2031 cm^{-1}, 1985 cm^{-1}).[34] When immobilized on the polymer-supported triphenylphosphine ligand, forming PS-TPP-**[Mn]**, carbonyl peaks were observed at 2086 cm^{-1}, 2000 cm^{-1}, 1952 cm^{-1} (Fig. 1, bottom) which are closely aligned with the mononuclear (homogeneous) *cis*-$MnBr(CO)_4(PPh_3)$ complex (2088 cm^{-1}, 2020 cm^{-1}, 2003 cm^{-1} and 1957 cm^{-1}).[35] These data are therefore consistent with the polymer containing a phosphorus-coordinated *cis*-$MnBr(CO)_4(PPh_3)$ group. In addition, solid-state ^{31}P NMR analysis of the free polymer-supported TPP ligand and polymer-supported Mn complex was carried out and a shift in the ^{31}P resonance was observed from −4.3 to 40.5 ppm,[35] which aligns with the corresponding resonance in the (homogeneous) *cis*-$MnBr(CO)_4(PPh_3)$ complex (for more details, see the SI).[36]

To evaluate the applicability of this catalyst, the hydrosilylation of esters to alcohols was examined.[13] Studies were initiated with PS-TPP-**[Mn]**, using methyl benzoate **1a** as a model substrate and phenylsilane at 100

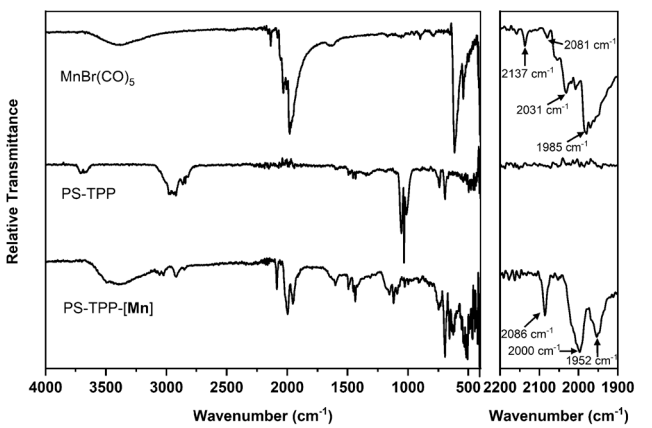

Fig. 1 ATR-FTIR analysis for $MnBr(CO)_5$ (top), PS-TTP (centre) and PS-TTP-**[Mn]** (bottom). The right-hand panel shows an expansion of the region between 2200 and 1900 cm^{-1}.

Table 1 Optimization of reaction conditions

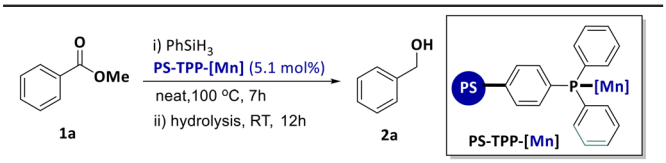

Entry	Deviation from standard condition	Yield (%)
1[a]	**Standard conditions**	76[b]
2	$MnBr(CO)_4PPh_3$ (homogeneous catalyst)	55[c]
3	$MnBr(CO)_5$	0
4	MnO or MnO_2 instead of PS-TPP-**[Mn]** catalyst	0
5	MnPc(II)	0
6	Using only PS-TPP (free polymer support)	0
7	Absence of PS-TPP-**[Mn]** catalyst	0
8	Absence of $PhSiH_3$	0
9	Benzaldehyde instead of **1a**	86[c]

[a] Unless otherwise noted, reaction conditions are as follows: i) **1a** (0.5 mmol), $PhSiH_3$ (1.0 mmol), PS-TPP-[Mn] (5.1 mol% Mn, 7.0 wt%), [Mn] = *cis*-$MnBr(CO)_4$ the neat reaction mixture was magnetically stirred at 100 °C for 7 h under air. ii) 10% NaOH (2 mL) and MeOH (3 mL) were added to the reaction mixture and stirred for 12 h at RT. [b] Isolated yields. [c] NMR yields using 1,3,5 trimethoxy benzene as an internal standard. PS-TPP = polymer supported Tri phenyl phosphine. MnPc(II) = manganese(II) phthalocyanine.

°C for 7 hours in air. Subsequent hydrolytic work-up yielded benzyl alcohol **2a** with a gratifying 76% yield on a 0.5 mmol scale (Table 1, entry 1). Deviating from our standard reaction conditions using PS-TPP-**[Mn]**, the homogeneous *cis*-$MnBr(CO)_4(PPh_3)$ complex gave a reduced yield (55%) of **2a** (Table 1, entry 2). No product was observed using commercially available $MnBr(CO)_5$ (*i.e.* in the absence of a phosphine ligand), suggesting that the phosphine ligand is crucial (Table 1, entries 3–5). In addition, a set of control experiments including the use of Mn-free polymer (PS-TPP), the absence of PS-TPP-**[Mn]**, and the absence of phenylsilane ($PhSiH_3$), (Table 1, entries 6–8) resulted in no formation of **2a**. In addition, the catalyst successfully reduced benzaldehyde affording **2a** in 86% yield (Table 1, entry 9).

With the optimal conditions established (Table 1, Entry 1), the substrate scope of esters was explored to evaluate the robustness of the heterogeneous Mn catalyst (Table 2). Methyl- and ethyl-esters (**1a** and **1b**) were efficiently reduced to **2a** in good yields (76 and 18%). Ester derivatives with a *p*-Me group (**1c** and **1d**) were very suitable substrates, producing corresponding benzyl alcohol product **2c** in decent yields (69 and 40%). Strongly electron-donating groups were also tolerated, and **1e** and **1f** were reduced to give the corresponding benzyl alcohols **2e** and **2f** in 53 and 89% yields. Halogenated substrates (**1g**–**1j**) also worked well

Table 2 Scope of ester and aldehyde reduction to alcohols using a polymer-supported manganese catalyst[a]

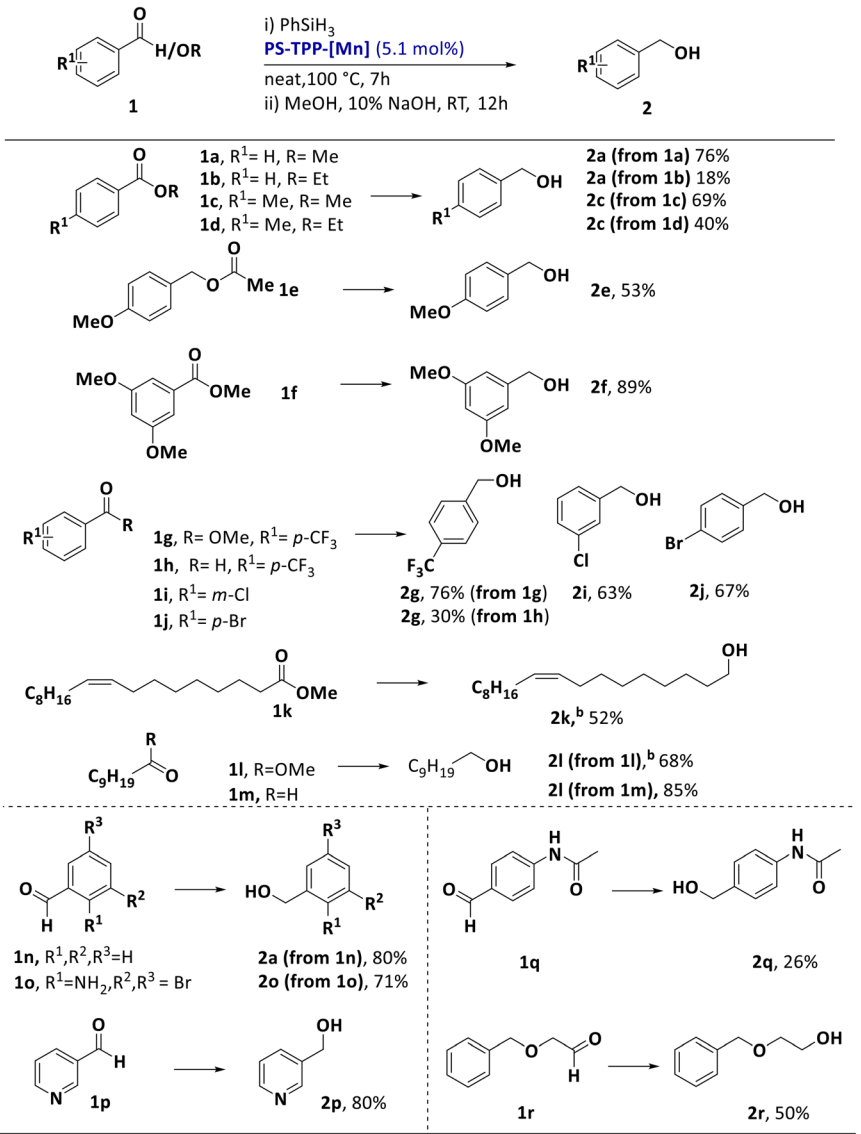

[a] Unless otherwise noted reaction conditions are as follows: i) **1a** (0.5 mmol), $PhSiH_3$ (1.0 mmol), PS-TPP-[Mn] (5.1 mol% Mn, 7.0 wt%), the neat reaction mixture was stirred at 100 °C for 7 h under air. ii) 10% NaOH and MeOH were added to the reaction mixture and stirred for 12 h at RT. Isolated yield using column chromatography on SiO_2. [b] $PhSiH_3$ (2.0 mmol) was used. PS-TPP = polymer supported triphenyl phosphine.

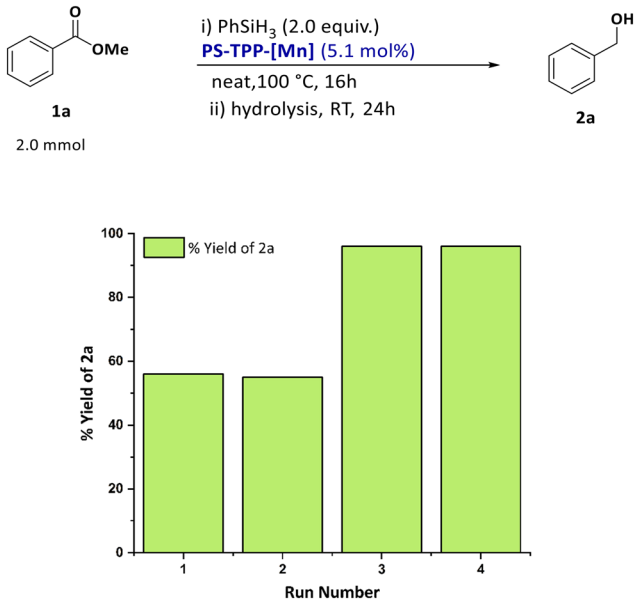

Scheme 2 Recyclability of PS-TPP-[Mn].

giving the desired products (**2g**–**2j**) in good yields (63–76%). In addition, aliphatic esters **1k** and **1l** were successfully reduced to the corresponding alcohols **2k** and **2l** using PS-TPP-[**Mn**] in 52% and 68% yields respectively. Turning to aldehydes, 4-(trifluoromethyl) benzaldehyde **1h** and decanal **1m** were successfully reduced to corresponding alcohols **2g** and **2l** in 30% and 85% yield under these conditions. Benzaldehyde was reduced to benzyl alcohol in 80% yield. Benzaldehyde substituted with Br and NH_2 groups **1o** could be transformed to the respective alcohol **2o** in 85% yield. Pyridinyl aldehyde **1p** was reduced to **2p** in 80% yield. Interestingly, an acetamide functional group was tolerated (**1q**) affording **2q** in 26%. Benzyl ether **1r** was reduced to **2r** in 50% yield.

Studies were then conducted to evaluate the reusability of the catalyst using **1a** (Scheme 2) at 2.0 mmol scale. We observed that the catalyst can be recycled and reused up to three times. Interestingly, the catalyst performance improved after the second recycle, giving a yield of **2a** in 96% yield. This prompted us to consider that a consequential change in catalyst structure was occurring during the reaction or on work-up (which involves a NaOH/MeOH wash).

To test if the catalyst could be 'primed' for higher activity, we took an unused batch of Mn catalyst and stirred it overnight in a saturated NaOH solution with MeOH (samples prepared in this manner are referred to as PS-TPP-[**Mn**]-**Primed**). The material was then isolated and tested in the standard reaction, under optimal reaction conditions. An improved yield (76%) of the reduced product, this time on a 2.0 mmol scale, was observed (Scheme 3).

Using the primed catalyst, a few substrates were re-examined. In addition to methyl benzoate **1a**, subtrates **1x** (*p*-methoxymethylbenzoate), **1t** (*p*-methoxybenzaldehyde) and **1v** (4-hydroxy-3-methoxybenzaldehyde (vanillin)) were used with both fresh and primed catalyst for comparison. Use of PS-TPP-[**Mn**]-**Primed** (NaOH/MeOH treatment) resulted in increased yields of product compared to an un-primed catalyst (**2a** from **1a**, 76 *vs.* 80%; **2e** from **1x**, 77 *vs.* 82%; **2e** from **1t**, 83 *vs.* 96%; **2v** from **1v**, 30% *vs.* 50%). While our results (using recyclized catalyst and primed catalyst) suggest a role of the base-wash to improve the catalyst efficiency, an extensive study involving normalised activity metrics is required to corroborate these observations and pinpoint the origin of any improved activity.

Primed Mn catalyst, PS-TPP-[**Mn**]-**primed**, was then used to reduce other esters and aldehydes (Table 3). Benzaldehydes with H, 4-Me, 4-OMe and 3,5-OMe (**1n**, **1s**, **1t** and **1u**) substitution were reduced efficiently using the primed catalyst in excellent yields (85, 93, 96 and 98%) to give **2a**, **2c**, **2e** and **2f** respectively. Vanillin **1v** was successfully reduced to give corresponding alcohol product **2v** in 50% yield. Esters **1w**, **1a**, **1x** and **1y** were reduced to give **2w**, **2a**, **2e** and **2y** respectively in 50, 80, 82 and 92% yield. Naphthalene ester **1z** was reduced to **2z** in 85% yield. The naproxen ester **1aa** gave

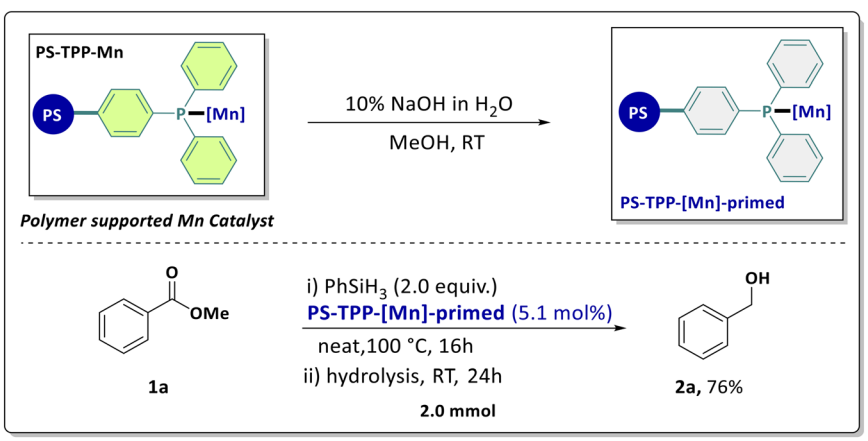

Scheme 3 Reduction using 'primed' heterogeneous Mn catalyst.

Table 3 Scope of ester and aldehyde reduction to alcohols using a polymer supported manganese catalyst[a]

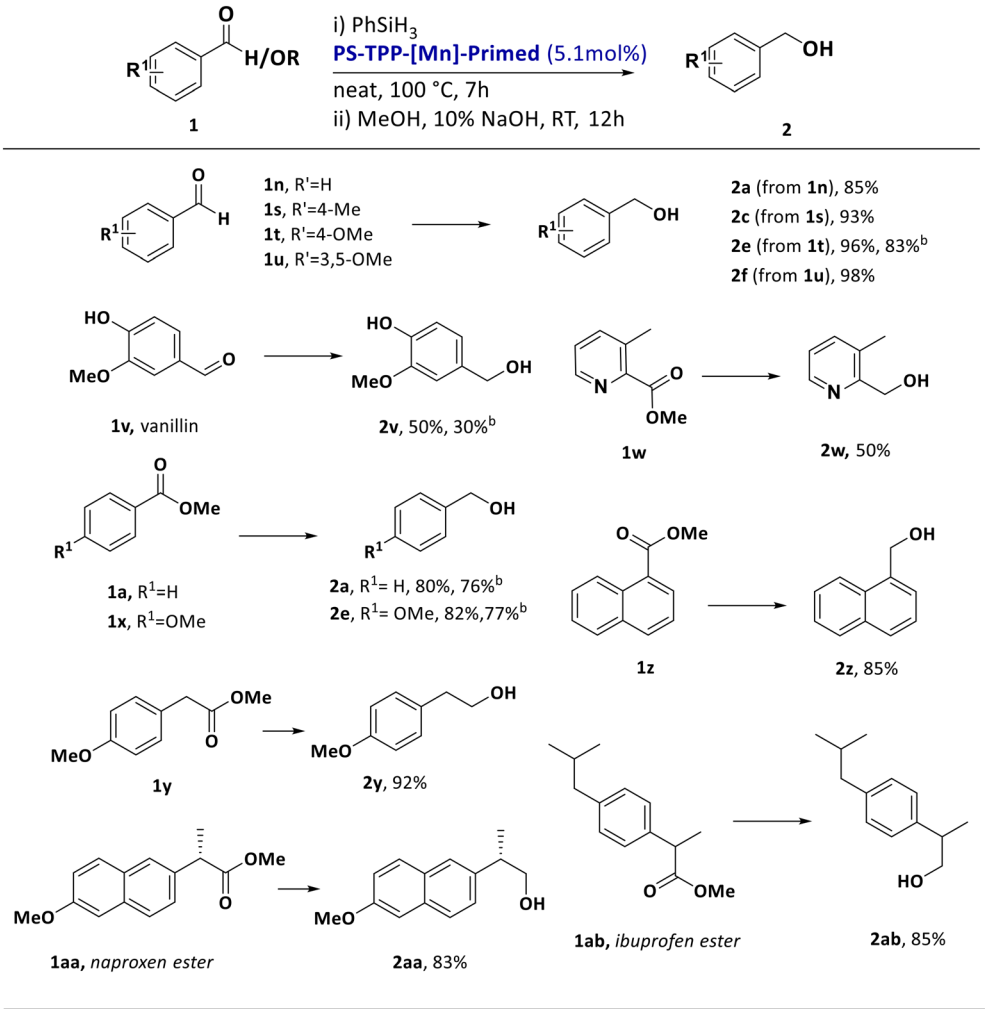

[a] Unless otherwise noted reaction conditions are as follows: i) **1a** (0.5 mmol), $PhSiH_3$ (1.0 mmol), PS-TPP-**[Mn]-Primed** (5.1 mol% Mn, 7.0 wt%), the neat reaction mixture was stirred at 100 °C for 7 h under air. ii) 10% NaOH and MeOH were added to the reaction mixture and stirred for 12 h at RT. Isolated yield using column chromatography on SiO_2. [b] Unprimed catalyst. PS-TPP = polymer supported triphenyl phosphine.

the corresponding alcohol **2aa** in 83% yield and finally Ibuprofen ester **1ab**, gave alcohol **2ab** in 85% yield. It is important to note that substrates **2e** (from **1t**), **2v** (from **1v**), **2a** (from **1a**), and **2e** (from **1x**) in Table 3 were also obtained using the un-primed catalyst and compared with the primed catalyst, which showed an increase in yield in all cases.

With a consistent trend showing improved yields when the primed catalyst was used, we turned our attention toward further analysis of this material. The FTIR spectra of *fresh* PS-TPP-**[Mn]** (Fig. 2, top), *primed* (NaOH) PS-TPP-**[Mn]-Primed** (Fig. 2, centre) and *recycled* PS-TPP-**[Mn]** (Fig. 2, bottom) were acquired. The intensity of the carbonyl peaks were significantly reduced in the primed catalyst compared to the fresh catalyst, and there was a change in band positions. No significant peaks corresponding to metal carbonyl vibrations were observed in the recycled catalyst (Fig. 2).

ICP-OES analysis revealed there was a minimal loss of Mn between the fresh and recycled or primed catalysts (for more details, see the SI). For example, the fresh Mn-based heterogeneous catalyst retained over 80% of the initial Mn content after recycling (some of this discrepancy possibly being in handling losses).[37]

Given the observation that the primed and recycled catalysts displayed reduced CO band intensity in the infrared spectra but enhanced reactivity, we then sought to understand changes to the Mn core during these processes. X-ray Absorption Fine Structure (XAFS) Spectroscopy provides information on the oxidation state and co-ordination environment of specific elements, in this case Mn. Fig. 3 shows the XAFS derived Mn K-edge energies of fresh PS-TPP-**[Mn]**, primed (NaOH) PS-TPP-**[Mn]-Primed** and used/recycled PS-TPP-**[Mn]** catalysts (as vertical dashed lines) along with reference compounds plotting oxidation state as a function of edge energy (all spectra given in the SI). It is commonly reported that the Mn oxidation state can be reliably estimated from edge shifts (solid foil/oxides

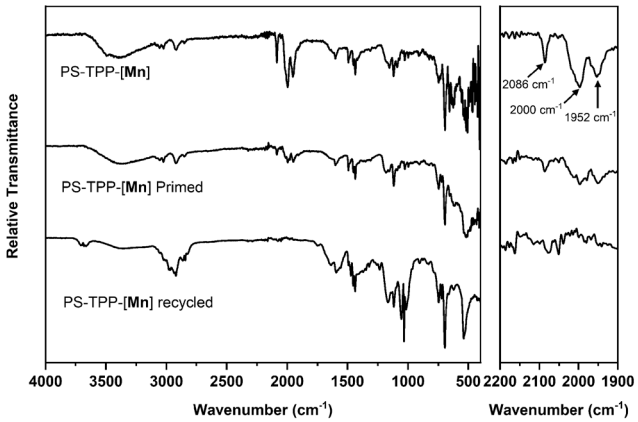

Fig. 2 FTIR analysis comparison of unused (top), primed (centre) and recycled (bottom) catalyst. The right-hand panel shows an expansion of the region between 2200 and 1900 cm^{-1}.

literature trendline shown on Fig. 3).[38,39] However, it is noted from the literature[40–42] and our own observations, that Mn(I) carbonyl compounds do not fit this trend. For similar materials, it is nevertheless expected that a shift to increased edge energies will still correspond to electron loss (oxidation) around the Mn centre, but that the absolute value of the formal oxidation state may be difficult to determine. It is clear that both priming and catalytic use (straight diagonal arrows in Fig. 3) result in a significant shift of the edge position to higher energies, indicative of reduced shielding of the core electron levels. The shape of the near-edge spectrum also changes (for more details, see the SI), highlighting differences in the electronic structure (typically associated with core to 4p excitation). The splitting pattern is sensitive to 3d orbital covalency, and therefore coordination, but difficult to ascribe precisely.[43,44] For our purposes it is most important to note that this change is seen in the primed and re-used catalyst and continues to occur in samples that have been used multiple times. It should also be noted that the reproducibility of this approach is attested to by the nearly co-incident values for two different batches of fresh PS-TPP-**[Mn]** in Fig. 3. The observed oxidation of Mn(I) to a slightly higher oxidation state seen here is unusual, however Beller does report a Mn(I) to Mn(II) oxidation (a disproportionation event) in the presence of H_2 mediated reduction.[45] Further studies to understand this phenomenon are being carried out in our laboratory.

SEM and EDX analyses were conducted (for more details, see the SI) on unused, primed, and recycled PS-TPP-**[Mn]** catalysts, revealing key insights (Fig. 4). Fresh and primed catalysts showed similar morphology with homogeneous distribution of Mn on the surface of the triphenyl phosphine polymer. In contrast, recycled catalysts fragmented into smaller particles, increasing surface area while maintaining Mn distribution and effectively exposing more Mn active sites for the reactants to interact. This structural transformation perhaps contributes to the

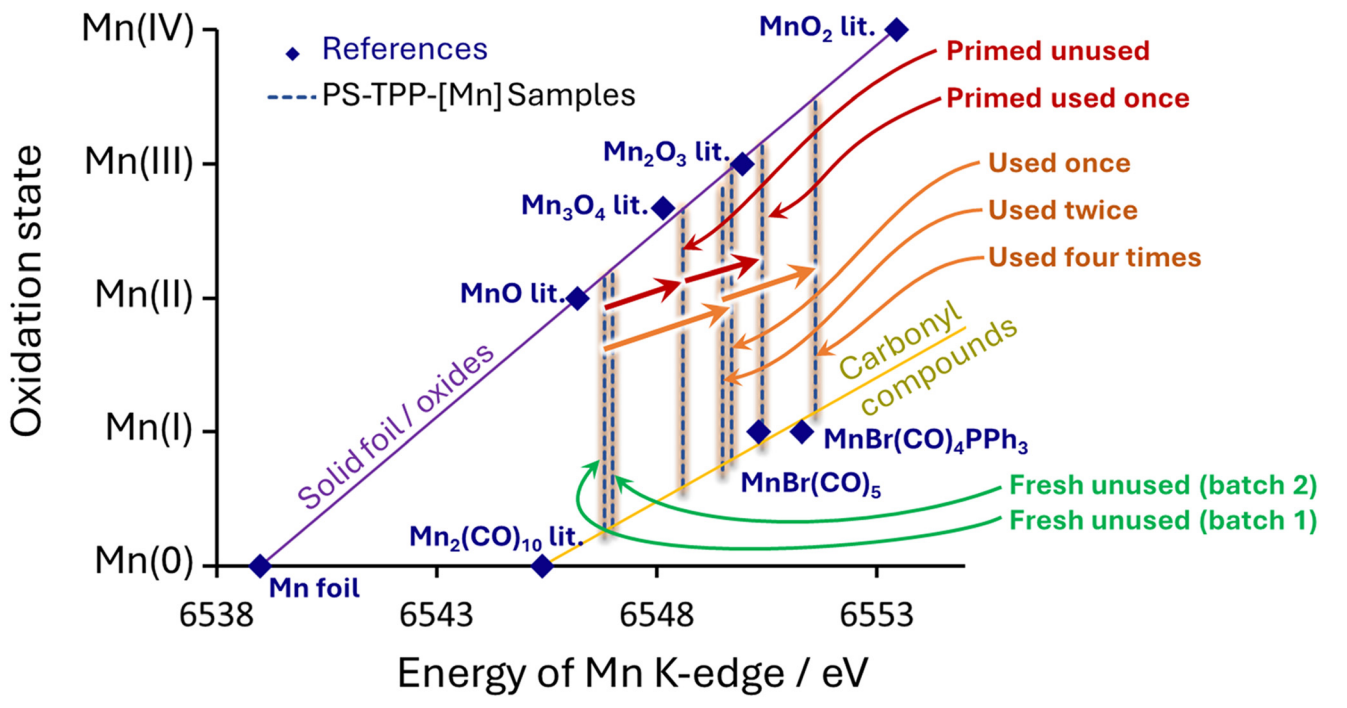

Fig. 3 A plot showing oxidation state *versus* the XAFS Mn K-edge position of several reference compounds, along with the position of fresh (green), primed (red) and used/recycled (orange) PS-TPP-**[Mn]** catalysts (shown as vertical dashed lines although anticipated to be Mn(I)). As a guide to the eye trendlines show the commonly reported trend for solid metal foil/oxides (purple), as well as for carbonyl compounds (mustard). The straight diagonal arrows highlight the primed *vs.* non-primed path – showing both priming and reuse increase the edge energy. While explicit oxidation states have been indicated, relative oxidation state changes lead to a more reliable interpretation.

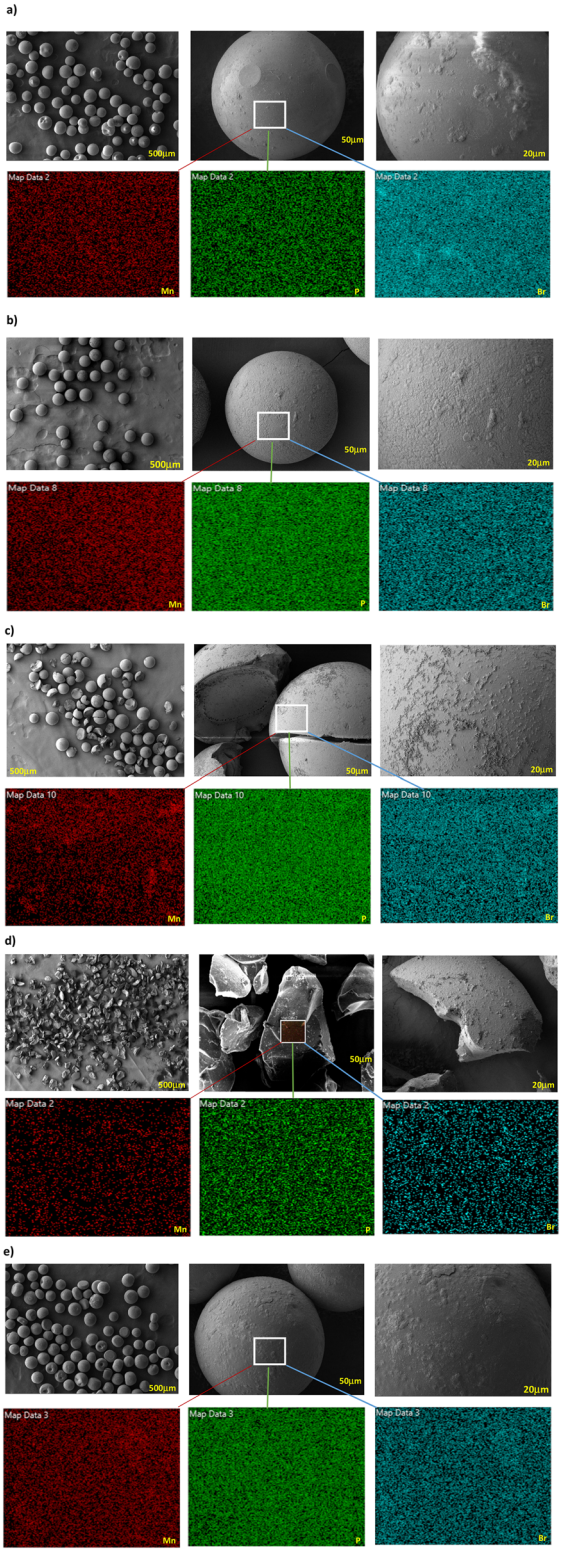

Fig. 4 Scanning electron microscopy and energy dispersive X-ray analysis. a) SEM and EDX analysis of fresh PS-TPP-[Mn] catalyst: surface distribution of Mn, P, and Br. b) SEM and EDX analysis of recycled PS-TPP-[Mn] catalyst (used once): surface distribution of Mn, P, and Br. c) SEM and EDX analysis of recycled PS-TPP-[Mn] catalyst (used twice): surface distribution of Mn, P, and Br. d) SEM and EDX of recycled PS-TPP-[Mn] catalyst (used four times): surface distribution of Mn, P, and Br. e) SEM and EDX analysis of PS-TPP-[Mn]-primed catalyst: surface distribution of Mn, P, and Br. Expansion boxes are not necessarily derived from the precise location shown.

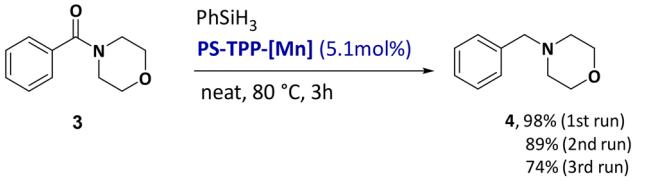

Scheme 4 Deoxygenation of amides to amines.

improved catalytic performance upon recycling. Sodium (Na) is retained on both the primed catalyst and the recycled catalyst (for more details, see the SI).

Finally, the heterogeneous Mn catalyst was next evaluated for the reduction of amides to their corresponding amines *via* deoxygenation. In 2017, Kelly *et al.* reported the reduction of amide carbonyl using a pre-synthesized homogeneous Mn catalyst,[46] whereas Huang *et al.* reported deoxygenation of amides to amines using homogeneous $MnBr(CO)_5$ under mild reaction conditions.[47] Using our heterogeneous catalyst, the reduction of amide **3** to amine **4** occurred in an excellent 98% yield (Scheme 4). The catalyst was further recycled and reused twice, achieving isolated yields of product **4** in 89% and 74% respectively.

Conclusion

In conclusion, we have designed and synthesized a polymer-supported heterogeneous manganese catalyst for selective transformation of organic carbonyl compounds (*i.e.*, esters and aldehydes) to the corresponding alcohols, and an amide to amine. We observed that the catalyst can be easily separated, recycled and reused. Unexpectedly, the recycled catalyst appears more active than that used in the first iteration, prompting analyses (FTIR, SEM, EDX, XAFS and ICP-OES) of the Mn catalyst before and after catalysis. The catalyst undergoes fragmentation, increasing its surface area and exposing more active Mn sites for hydrosilylation. In addition, changes in the Mn oxidation state (increasing upon recycling or priming) were observed from initial use. These insights led us to develop a priming procedure to provide a highly active and viable catalyst. At this stage it is unclear the respective roles that Mn oxidation and catalyst fragmentation play in catalyst activity. An in-depth quantitative study is required, and further investigations to broaden the application of this heterogeneous Mn catalyst and opportunities for synthesis are currently underway in our laboratory.

Conflicts of interest

There are no conflicts to declare.

Data availability

The data underlying this manuscript is available in the published supplementary information (SI), including experimental details, NMR spectra, SEM EDX and XAFS data.

Supplementary information is available. See DOI: https://doi.org/10.1039/d5cy01174d.

Acknowledgements

The authors would like to acknowledge Research Ireland (previously the Irish Research Council and Science Foundation Ireland (21/FFP-A/8784)), the Synthesis and Solid-State Pharmaceutical Centre (SSPC) (SFI/12/RC/2275_P2) and a research infrastructure award for process flow spectroscopy (ProSpect, grant: 15/RI/3221 and 21/RI/9705) and the EPSRC (grant number EP/W031914/1) for funding. We acknowledge Durham University's XAFS facility, supported by the Engineering and Physical Sciences Research Council [grant number EP/V029053/1]. We thank Dr Niall Donaldson at the University of York for ICP analysis. We thank the STFC for programme access to the ULTRA facility (grant number 1813). JML and IJSF are both supported by Royal Society Industry Fellowships (INF\R1\221057 and INF\R2\202122 respectively). We are grateful to Denis Lynch (UCC) for assistance with NMR spectroscopy. We are grateful to Dr Michael Schmidt from Tyndall National Institute for SEM-EDX analysis. We would like to thank Dr Manuel Ruether (TCD) for solid state phosphorus NMR analysis.

References

1 R. Giri, B.-F. Shi, K. M. Engle, N. Maugel and J.-Q. Yu, *Chem. Soc. Rev.*, 2009, **38**, 3242–3272.
2 *Catalysis with Earth-abundant Elements*, ed. U. Schneider and S. Thomas, The Royal Society of Chemistry, 2020.
3 K. J. Kadassery, S. N. MacMillan and D. C. Lacy, *Inorg. Chem.*, 2019, **58**, 10527–10535.
4 P. Chen, J. B. Bornhorst and M. Aschner, *Front. Biosci.-Landmark*, 2018, **23**, 1655–1679.
5 K. S. Egorova and V. P. Ananikov, *Organometallics*, 2017, **36**, 4071–4090.
6 Y. Hu, B. Zhou and C. Wang, *Acc. Chem. Res.*, 2018, **51**, 816–827.
7 W. Liu and L. Ackermann, *ACS Catal.*, 2016, **6**, 3743–3752.
8 C. Miao, X.-X. Li, Y.-M. Lee, C. Xia, Y. Wang, W. Nam and W. Sun, *Chem. Sci.*, 2017, **8**, 7476–7482.
9 R. Cano, K. Mackey and G. P. McGlacken, *Catal. Sci. Technol.*, 2018, **8**, 1251–1266.
10 N. Ahmed, *J. Organomet. Chem.*, 2024, **1009**, 123071.
11 K. Das, S. Waiba, A. Jana and B. Maji, *Chem. Soc. Rev.*, 2022, **51**, 4386–4464.
12 P. W. Schlichter Christophe, *Synthesis*, 2021, **54**, 517–534.
13 R. R. Behera, R. Ghosh, S. Panda, S. Khamari and B. Bagh, *Org. Lett.*, 2020, **22**, 3642–3648.
14 O. Martínez-Ferraté, B. Chatterjee, C. Werlé and W. Leitner, *Catal. Sci. Technol.*, 2019, **9**, 6370–6378.
15 Z. Mao, B. T. Gregg and A. R. Cutler, *J. Am. Chem. Soc.*, 1995, **117**, 10139–10140.
16 T. K. Mukhopadhyay, C. L. Rock, M. Hong, D. C. Ashley, T. L. Groy, M.-H. Baik and R. J. Trovitch, *J. Am. Chem. Soc.*, 2017, **139**, 4901–4915.
17 J. K. Pagano, J. M. Dorhout, R. Waterman, K. R. Czerwinski and J. L. Kiplinger, *Chem. Commun.*, 2015, **51**, 17379–17381.
18 M. Schmal, *Heterogeneous Catalysis and its Industrial Applications*, 2016.
19 Z. Li, S. Ji, Y. Liu, X. Cao, S. Tian, Y. Chen, Z. Niu and Y. Li, *Chem. Rev.*, 2020, **120**, 623–682.
20 X. Cui, W. Li, P. Ryabchuk, K. Junge and M. Beller, *Nat. Catal.*, 2018, **1**, 385–397.
21 F. Ferlin, A. Marini, N. Ascani, L. Ackermann, D. Lanari and L. Vaccaro, *ChemCatChem*, 2020, **12**, 449–454.
22 K. Yamaguchi, Y. Wang and N. Mizuno, *ChemCatChem*, 2013, **5**, 2835–2838.
23 N. E. Leadbeater and M. Marco, *Chem. Rev.*, 2002, **102**, 3217–3274.
24 C. H. Raksha, M. P. Yogeesh and N. S. Shetty, *Discover Appl. Sci.*, 2025, **7**, 565.
25 P. Vimal, C. P. Babu Rajeev, N. Javeed, G. Periyasamy and V. Gayathri, *J. Catal.*, 2025, **447**, 116113.
26 A. Sen, T. Sato, A. Ohno, H. Baek, A. Muranaka and Y. M. A. Yamada, *JACS Au*, 2021, **1**, 2080–2087.
27 J. Lin, D. Song, W. Zhang, C. Zheng, C. Zheng, J. Lv, J. Xue, W. Zhong and F. Ling, *Green Chem.*, 2025, **27**, 8251–8259.
28 Y. Wang, M. Jiang, T. Tian, Z. Sun, G. Wu, Y. Wang, X. Guo, W. He, J. Ding, L. Yan and Y. Ding, *Mol. Catal.*, 2024, **567**, 114459.
29 I. Choi, Z. Shen, E. Ronge, V. Karius, C. Jooss and L. Ackermann, *Chem. - Eur. J.*, 2021, **27**, 12737–12741.
30 P. He, B. Chen, L. Huang, X. Liu, J. Qin, Z. Zhang and W. Dai, *Chem*, 2022, **8**, 1906–1927.
31 B. Wang, J. Lin, C. Xia and W. Sun, *J. Catal.*, 2022, **406**, 87–95.
32 X. Liu, B. Han, C. Wu, P. Zhou, M. Jia, L. Zhu and Z. Zhang, *Angew. Chem., Int. Ed.*, 2025, **64**, e202413799.
33 R. J. Angelici and Fred. Basolo, *J. Am. Chem. Soc.*, 1962, **84**, 2495–2499.
34 T. Vielhaber and C. Topf, *Appl. Catal., A*, 2021, **623**, 118280.
35 B. R. O'Donoghue, S. Flesch, E. Courtney, S. Choudhary, J. B. Eastwood, K. Mackey, L. M. Pardo, I. P. Clark, P. Malakar, G. M. Greetham, A. C. Whitwood, R. J. Gammons, G. P. McGlacken, I. J. S. Fairlamb and J. M. Lynam, *Inorg. Chem.*, 2025, **64**, 16768–16780.
36 E. Lindner, R. Fawzi, H. A. Mayer, K. Eichele and K. Pohmer, *Inorg. Chem.*, 1991, **30**, 1102–1107.
37 C. S. Horbaczewskyj and I. J. S. Fairlamb, *Org. Process Res. Dev.*, 2022, **26**, 2240–2269.
38 J. Zenner, K. Tran, L. Kang, N. W. Kinzel, C. Werlé, S. DeBeer, A. Bordet and W. Leitner, *Chem. – Eur. J.*, 2024, **30**, e202304228.
39 T. Ressler, J. Wong, J. Roos and I. L. Smith, *Environ. Sci. Technol.*, 2000, **34**, 950–958.
40 S. Khabuanchalad, J. Wittayakun, R. J. Lobo-Lapidus, S. Stoll, R. D. Britt and B. C. Gates, *Langmuir*, 2013, **29**, 6279–6286.

41 S. Khabuanchalad, J. Wittayakun, R. Lobo-Lapidus, S. Stoll, R. Britt and B. Gates, *J. Phys. Chem. C*, 2010, **114**, 17212–17221.
42 J. M. Ramallo-López, E. J. Lede, F. G. Requejo, J. A. Rodriguez, J.-Y. Kim, R. Rosas-Salas and J. M. Domínguez, *J. Phys. Chem. B*, 2004, **108**, 20005–20010.
43 F. Bridges, C. H. Booth, M. Anderson, G. H. Kwei, J. J. Neumeier, J. Snyder, J. Mitchell, J. S. Gardner and E. Brosha, *Phys. Rev. B: Condens. Matter Mater. Phys.*, 2001, **63**, 214405.
44 M. Croft, D. Sills, M. Greenblatt, C. Lee, S.-W. Cheong, K. V. Ramanujachary and D. Tran, *Phys. Rev. B: Condens. Matter Mater. Phys.*, 1997, **55**, 8726–8732.
45 V. Papa, Y. Cao, A. Spannenberg, K. Junge and M. Beller, *Nat. Catal.*, 2020, **3**, 135–142.
46 C. M. Kelly, R. McDonald, O. L. Sydora, M. Stradiotto and L. Turculet, *Angew. Chem., Int. Ed.*, 2017, **56**, 15901–15904.
47 J. Huang, F. Sun and W. Liu, *J. Catal.*, 2023, **423**, 19–25.